Effects of disorder in ferroelastics: A spin model for strain glass

Romain Vasseur[1,2] and Turab Lookman[1]

[1]*Theoretical Division and Center for Nonlinear Studies, Los Alamos National Laboratory, Los Alamos, New Mexico 87545, USA*
[2]*École Normale Supérieure de Lyon, 46 Allée d'Italie, 69007 Lyon, France*
(Received 11 February 2010; published 15 March 2010)

We demonstrate that a strain pseudospin model for martensitic alloys predicts a glass phase in the presence of disorder, consistent with recent experiments on binary and ternary alloys that have established the existence of such a phase above a critical composition. We find that the glass phase, as characterized by the Edwards-Anderson order parameter, exists even in the absence of elastic long-range interactions, which compete with the disorder to shift the glass transition to higher values of disorder. Our model predicts a second-order phase transition between the martensite and strain glass phases as a function of the disorder. Together with the cusp in the susceptibility and the history dependence in the glass phase in zero-field-cooling and field-cooling curves, these predictions may be tested experimentally by varying the alloy composition. Our approach using mean-field analysis and Monte Carlo simulations may be generalized to the study of glassy behavior in more complex structural transformations in two and three dimensions.

I. INTRODUCTION

Recent experiments on ferroelastic alloys have established the existence of a martensite or "strain" glass phase[1] in which localized random configurations of lattice distortions are kinetically frozen below a glass transition temperature, T_g. This glass phase was initially observed in Ni-rich $Ti_{50-x}Ni_{50+x}$ where the austenitic $B2$ parent structure appeared to persist to 0 K above a compositional threshold $x > 1.3$, below which it transformed to a martensitic $B19'$ phase. The strain glass has now been identified in numerous alloys and the means by which it is derived—by doping point defects or compositional variations beyond a critical value—makes it analogous to the well-known frozen disorder and frustration demonstrated in other ferroic systems such as magnetic spins in a spin glass[2] or electric dipoles in a ferroelectric relaxor.[3] The "nonmartensitic" strain glass exhibits unique features such as the shape-memory effect and pseudoelasticity, which are typical of alloys undergoing martensitic transitions. Moreover, the pretransitional "tweed" phase that can exist over a wide temperature range (∼100 K) above the martensitic transition, shows no glass-like response in the frequency dispersion of the storage modulus and internal friction or history dependence in the zero-field-cooling (ZFC)/field-cooling (FC) curves.[1,4] The tweed phase, which shows short-range strain order in an otherwise globally disordered system, was conjectured to be a spin glass.[5–8]

Our objective is to demonstrate how the strain glass phase emerges from a strain pseudospin model of a ferroelastic martensite. We predict this phase analytically using mean-field theory and obtain the phase diagram for the austenite-martensite-glass system. Our results are supported by numerical simulations, that include long-range elastic interactions on the full model, and are consistent with the salient aspects of experiments which have led theoretical advances in this field. Numerical studies[9] on continuum models with long-range interactions and disorder tend not to be predictive as they do not consider an order parameter (OP) that charac-terizes the glass phase. We show that the long-range elastic interaction is not required to obtain the glass phase, but it competes with the disorder to suppress it so that the glass transition is shifted to larger values of the disorder. Our model also predicts a second-order phase transition between the martensite ground state and strain glass phase that could be tested experimentally.

Our starting point is a recently proposed strain pseudospin model for a square to rectangle martensitic transformation in two dimensions (2D).[10] This is the simplest in a class of clock models that can be defined for various ferroelastic materials undergoing a first-order structural transition with accompanying softening in the shear modulus. The models describe faithfully the martensitic domain microstructures in both two dimensions and three dimensions (3D),[10,11] such as twins for the square to rectangle and nested star microstructure for the triangle to centered rectangle in 2D, and can be derived systematically from the corresponding continuum models in which the strain components are the order parameters. By adding disorder to this model we relate our work to the usual spin-glass models.[12–15] A recent perspective[8] on spin-glass models for martensitic alloys, and in particular the tweed phase, emphasizes that oversimplified spin models can potentially miss the salient features of these alloys.

Our pseudospin Hamiltonian is a Blume-Capel[16] model with temperature-dependent coefficients and long-range interactions. This spin model predicts the twinned martensite phase at low temperature without disorder. Adding fluctuations to the transition temperature[6] in continuum models typically leads to the tweed precursor phase. Our model considers disorder through the coefficients in the Hamiltonian, rather than through the transition temperature itself. We assume a Gaussian distribution with nonzero temperature-dependent mean for both the crystal field and the exchange interactions. Moreover, for the sake of simplicity, we consider the disorder in the coefficients of the pseudospin Hamiltonian to be such that there is no correlation between their Gaussian distributions. The coefficients are functions of the temperature and thus the model is a generalization of the Ghatak-Sherrington model[14] but, in addition, also includes

long-range interactions. We also analyze the influence of a random local stress field. The models are studied within the Edwards-Anderson[12] mean-field theory in the limit of vanishing long-range interactions. We compare our results to Monte Carlo simulations and also numerically analyze the role of the long-range interactions.

II. SPIN-GLASS MODEL

Displacive (group↔subgroup) martensites can be driven by shear strains and/or shuffle (or displacement) modes. If the primary order parameters are strains, we have the so-called proper martensites, whereas if they are shuffles, we have the improper martensites. The shape-memory alloys $Fe_{1-x}Pd_x$, InTl, VSi, as well as CuAlNi are some of the examples of martensites where the primary mechanism is shear softening. We have chosen FePd as our example. Measurements by Muto *et al.*[17] of the elastic properties have shown that $C' = (1/2)(C_{11} - C_{12})$ softens as a function of temperature in FePd. It is a partial softening, the first-order transition temperature occurs at a temperature higher than the fictitious temperature at which C' would become zero, which is the stability limit of the austenite. In addition, these temperatures for FePd depend on the relative composition x. Based on the experimental data in Ref. 17, a Landau functional based on shear strains for FePd was parametrized in Ref. 18. Moreover, Barsch[19] also considered the improper martensitic (shuffle or phonon-driven) transformations in AuCd and NiTi, so that there is ample evidence for both shear and shuffle transformations in martensites. In fact, in some of the shuffle-based martensites (such as NiTi, see Ref. 20) there is a concomitant shear strain as well. Over the last twenty years an extensive literature on shear-driven martensites has been established, including the use of Landau theory, and we refer to contributions by Falk, Krumhansl, Barsch, Jacobs, and many others (see also Ref. 21). A review of the data and theory as pertaining to InTl has also been given by Saunders.[22] The spin model we discuss is appropriate for the shear-driven transformations, for materials such as FePd, InTl, and VSi which undergo a cubic-to-tetragonal transformation, where the nature of the driving mechanism is well established. Moreover, we will illustrate our ideas with reference to the two-dimensional square to rectangle transition for FePd as generalization to 3D is straight forward without conceptual difficulties. The transition is driven by the deviatoric strain $e_2 = 1/\sqrt{2}(\varepsilon_{11} - \varepsilon_{22})$, which serves as the OP, where $\varepsilon_{ij} = \frac{1}{2}(\frac{\partial u_i}{\partial x_j} + \frac{\partial u_j}{\partial x_i})$ are the components of the Lagrangian strain tensor. The bulk dilatation strain $e_1 = 1/\sqrt{2}(\varepsilon_{11} + \varepsilon_{22})$ and the shear strain $e_3 = \epsilon_{12}$ are the two non-OP symmetry-adapted strains.

The free-energy density is a sum of three contributions: $f = f_L(e_2) + f_G(\nabla e_2) + F_{non\text{-}OP}(e_1, e_3)$ with Landau free energy $f_L[e_2(\vec{r})]/E_0 = (\tau - 1)e_2^2 + e_2^2(e_2^2 - 1)^2$, where $\tau = \frac{T - T_c}{T_o - T_c}$ is the scaled temperature, T_o is the transition temperature, and T_c the temperature of the austenite stability limit. For $\tau < 4/3$, the uniform-martensite solutions are the two variants $\pm \varepsilon(\tau)$, where $\varepsilon^2(\tau) = 2/3(1 + \sqrt{1 - 3\tau/4})$.[10] The energy cost for interfaces, $f_G[e_2(\vec{r})]/E_0 = \xi^2 |\nabla e_2|^2$, is the usual Ginzburg term

with ξ the interfacial energy cost and E_0 an energy scale factor. The energy for the non-OP strains $f_{non\text{-}OP}/E_0 = 1/2[A_1 e_1^2 + A_3 e_3^2]$, where A_1 and A_3 are bulk and shear moduli, respectively, can be expressed as $f_{non\text{-}OP}/E_0 = A_1/2 \int d\vec{r}' e_2(\vec{r}) U(\vec{r} - \vec{r}') e_2(\vec{r}')$ using the strain compatibility relation $\nabla \times (\nabla \times \underline{\varepsilon})^T = 0$ as the three strains e_1, e_2, and e_3 are not independent[6,21,23] but are derivatives of two displacement components. The kernel $U(\vec{r} - \vec{r}')$ is a long-range repulsive potential that is anisotropic and decays as $1/r^2$ and is given in Fourier space by $U(k) = (k_x^2 - k_y^2)^2/(k^4 + 8\frac{A_1}{A_3}k_x^2 k_y^2)$. Thus, microstructure with orientations along diagonals $k_x = \pm k_y$ is favored and it is the bulk modulus, A_1, that controls the strength of the long-range interaction. We introduce the approximation $e_2(\vec{r}) \rightarrow \varepsilon(\tau)S(\vec{r})$, where the pseudospin $S(\vec{r})$ has the value $S(\vec{r}) = 0, \pm 1$ so that the associated pseudospin Hamiltonian obtained from the free energy, f, equivalent to a classical spin-1 Blume-Capel model[16] is

$$\beta H = \frac{D_0}{2}\left\{\sum_{i=1}^{N}[g_0 S_i^2 + \xi^2(\nabla S_i)^2] + \frac{A_1}{2}\sum_{i,j}U_{i,j}S_i S_j\right\}, \quad (1)$$

where $U_{i,j} = U(\vec{r}_i - \vec{r}_j)$, $D_0 = 2E_0\varepsilon^2/T$, $\beta = 1/T$, and $g_0(\tau) = (\tau - 1) + (\varepsilon^2 - 1)^2$. The gradient term is to be understood as a finite-difference operator that can be expressed in terms of $S_i S_j$. The spin approximation reduces the degrees of freedom of the system and mean-field and Monte Carlo simulations of the Hamiltonian (1) using the Metropolis method with periodic boundary conditions give rise to twins with sharp domain walls oriented along the diagonal. Thus this discrete spin model as well as similar models for other structural transformations involving more minima are able to reproduce the results of complex microstructure typically obtained using continuum relaxation dynamics.[11]

We remark that the reference state for the Landau theory is the high-symmetry phase (square in our two-dimensional model). The elastic moduli in the energy are for the high-symmetry phase and at the martensitic temperature, there is an instability and the appropriate temperature-dependent elastic modulus C', with reference to the high-symmetry phase, is no longer defined. This is because the system has transformed to the stable martensite phase (the rectangle in our model). However, the transformed phase is perfectly stable with a well-defined elastic modulus of its own. Numerous studies using our continuum models, as well as other phase-field approaches, have obtained the transformed microstructure with well-defined elastic properties. The minima of the wells correspond to the martensite variants. These minima have well-defined strains (with reference to the high-symmetry phase) obtained from the original free energy. To see that they have well-defined elastic properties, one can expand the energy functional, in terms of the strains within the wells, centered about the minimum. The elastic modulus at the harmonic level for the homogeneous low-symmetry variant, at the minimum, could then be written in terms of combinations of parameters (e.g., second-order and higher order elastic constants) for the high-symmetry phase. In addition, one could also take the microstructure obtained from the model and apply an external stress and obtain the elastic properties that way. So the model is well defined and there is

no problem in the use of this model to obtain microstructure that also has well-defined elastic properties. This also holds for the discrete version of the above model. We obtain the correct martensite microstructure with the "discrete wells" and the mapping (as for the ϕ^4 Ising theory) is therefore a good approximation, given that we are reducing the degrees of freedom. The key point is also that the instability is still with respect to the parent, high-symmetry phase, but the strains (or spins) of the transformed phase are well defined. The elastic modulus of the transformed microstructure or for a single variant may also be obtained by applying an external field. Thus, there is again no difficulty in the use of this model with the given definition of the spins. The coefficient of the S^2 term is inherited from the Landau potential and this encodes "effective elastic" properties at the discrete level.

In order to study the influence of disorder, we first consider the pseudospin Hamiltonian (1) in the limit $A_1=0$. The effects of the long-range interaction will be studied with Monte Carlo simulations. Hamiltonian (1) can be recast into a usual Blume-Capel or Blume-Emery-Griffiths Hamiltonian[16] with temperature-dependent coefficients $H=-J_0(\tau)\sum_{\langle i,j\rangle}S_iS_j+\Delta_0(\tau)\sum_iS_i^2$, where $\Delta_0=D_0(\tau)/(2\beta)[g_0(\tau)+4\xi^2]$ and $J_0=D_0(\tau)\xi^2/\beta$. The first sum runs over all pairs of nearest neighbors and the Hamiltonian has a first-order phase transition for $\tau=1$, corresponding to the austenite/martensite transformation. In order to include disorder in the model, we propose the Hamiltonian

$$H = - \sum_{\langle i,j\rangle} J_{ij}(\tau)S_iS_j + \sum_i \Delta_i(\tau)S_i^2, \quad (2)$$

where the J_{ij}'s and Δ_i's are distributed according to two independent, temperature-dependent, Gaussian distributions with respective means $[J_0(\tau),\Delta_0(\tau)]$ and variances $(\sigma_J^2,\sigma_\Delta^2)$

$$\mathcal{P}(J_{ij}) = \frac{1}{\sqrt{2\pi}\sigma_J}\exp\left\{-\frac{[J_{ij}-J_0(\tau)]^2}{2\sigma_J^2}\right\}, \quad (3)$$

$$\mathcal{P}(\Delta_i) = \frac{1}{\sqrt{2\pi}\sigma_\Delta}\exp\left\{-\frac{[\Delta_i-\Delta_0(\tau)]^2}{2\sigma_\Delta^2}\right\}. \quad (4)$$

We study the model within equilibrium statistical mechanics and average the free energy over the disorder distribution. As disorder is typically included by adding randomness in the transition temperature, an improved version of our model would thus consider correlations between the two distributions. For the sake of simplicity, we only consider independent distributions. We note that Hamiltonians that contains temperature-dependent coefficients have been previously studied, in particular, the ϕ^4 field theory with temperature-dependent coefficients and the discrete Ising model with temperature-dependent interactions.[24] These Hamiltonians have been investigated without the need for any special treatment—the statistical averages are performed in the usual way, the partition function is a functional integral of the Boltzmann weight $\exp(-\beta H_{eff}[\phi])$, and the Landau mean-field approximation is a saddle-point approximation to this integral.

III. MEAN-FIELD PHASE DIAGRAM

We calculate the mean-field free energy of this model using the replica method and the derivation is closely analogous to that of the Sherrington-Ghatak (SG) model.[14] However, our model has Δ random and a nonzero J_0 that yields a ferromagnetic/martensite phase, in addition to the paramagnetic/austenite phase. Moreover, the mean values J_0 and Δ_0 are functions of the temperature, this is necessary to obtain the correct first-order transition for $\tau=1$ when there is no disorder. Even for $A_1=0$, this problem is complex and requires three different order parameters. One can recover the results of the SG model in the limit $\sigma_\Delta\to0$ and $J_0\to0$. Using the replica trick identity $\ln Z=\lim_{n\to0}(Z^n-1)/n$, standard calculations yield the mean-field free energy, the detailed calculations are given in the Appendix. The trace for the replicated system cannot be performed exactly and therefore we introduce three mean-field parameters $m^\alpha=\langle S_i^\alpha\rangle_n$, $p^\alpha=\langle S_{i\alpha}^2\rangle_n$, and $q^{\alpha\beta}=\langle S_i^\alpha S_i^\beta\rangle_n(\alpha\neq\beta)$, where the brackets indicate statistical averages and where α and β label n dummy replicas. We further make the usual replica ansatz that all the m's, q's, and p's have the same value at the extremum of the free energy. We dot not consider the replica-symmetry-breaking scheme here.[15,25,26] The mean-field free energy is

$$f(m,p,q) = \frac{J_0z}{2}m^2 + \frac{\beta^2\sigma_J^2z}{4}(p^2 - q^2)$$
$$- T\int \frac{dxdy}{2\pi}e^{-r^2/2}\ln(1 + 2e^\alpha\cosh\gamma), \quad (5)$$

where z is the number of nearest neighbors and $r^2=x^2+y^2$, $\alpha(y)=\frac{\beta^2\sigma_J^2z}{2}(p-q)-\beta(\Delta_0+\sigma_\Delta y)$ and $\gamma(x)=\beta\sigma_Jx\sqrt{zq}+\beta J_0zm$. Mean-field self-consistency equations can be obtained by minimizing the free energy Eq. (5)

$$m = \int \frac{dxdy}{2\pi}e^{-(x^2+y^2)/2}\frac{2\sinh\gamma}{e^{-\alpha}+2\cosh\gamma},$$

$$p = \int \frac{dxdy}{2\pi}e^{-(x^2+y^2)/2}\frac{2\cosh\gamma}{e^{-\alpha}+2\cosh\gamma}, \quad (6)$$

$$q = p - \frac{1}{\zeta}\int \frac{dxdy}{2\pi}e^{-(x^2+y^2)/2}\frac{2x\sinh\gamma}{e^{-\alpha}+2\cosh\gamma}$$

with $\zeta=\beta J\sqrt{zq}$.

The solution of the coupled Eq. (6) gives the phase diagram of the original random system shown in Fig. 1. In the original system, $m=\overline{\langle S\rangle}$, $q=\overline{\langle S\rangle^2}$, and $p=\overline{\langle S^2\rangle}$, where the bar refers to an average over the disorder. In addition to the two usual martensite ($m\neq0,q=0$) and austenite ($m=0,q=0$) phases, separated by a first-order transition, we predict a spin-glass phase ($m=0,q\neq0$) characterized by the EA order parameter[12] q. The value of the variance σ_Δ is not relevant to the topology of the phase diagram, only σ_J is important for the existence of the spin-glass phase. The salient features in Fig. 1 are in good, qualitative agreement with the experimental phase diagram[1] on strain glasses. The susceptibility curves in Fig. 2 show signatures of both the first-order and second-order transitions. The susceptibility is obtained
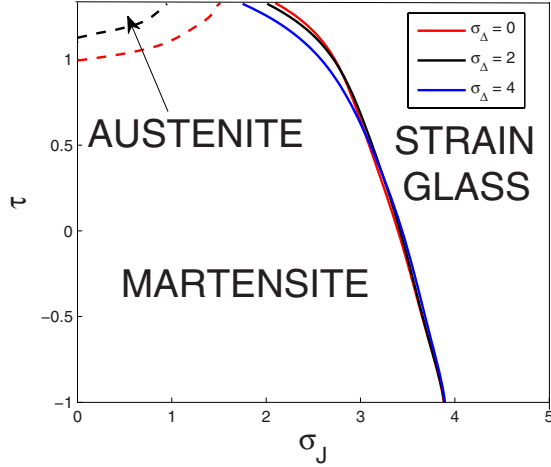
FIG. 1. (Color online) Mean-field phase diagram of the random Hamiltonian (2) in the plane (τ, σ_J) for different values of disorder characterized by variance σ_Δ. Dashed lines correspond to first-order phase transitions and solid lines to second-order transitions. The three phases are: austenite (paramagnetic, $m=0$, $q=0$), martensite (ferromagnetic, $m \neq 0$, $q \neq 0$), and strain glass (spin glass, $m=0$, $q \neq 0$). For large values of σ_Δ the first-order line between austenite and martensite vanishes. We found no glassy phase for $\sigma_J=0$ even for large values of σ_Δ.

from the fluctuation-dissipation relation $\chi \equiv \lim_{h \to 0} \frac{\partial m}{\partial h} = \beta(\langle S^2 \rangle - \langle S \rangle^2) = \beta(p-q)$. For small values of the disorder σ_J, there is a jump in these curves corresponding to the first-order phase transition between the austenite and the martensite phases. As the disorder is increased, this peak shifts to higher temperatures and then vanishes beyond the limiting temperature $\tau=4/3$. For higher temperatures, the susceptibility shows a cusp at the second-order phase transition between the spin-glass phase and the low-temperature ferromagnetic or martensite phase. This cusp is the signature of a glassy transition[2,27] that could be measured experimentally by studying the elastic properties of martensitic alloys as a
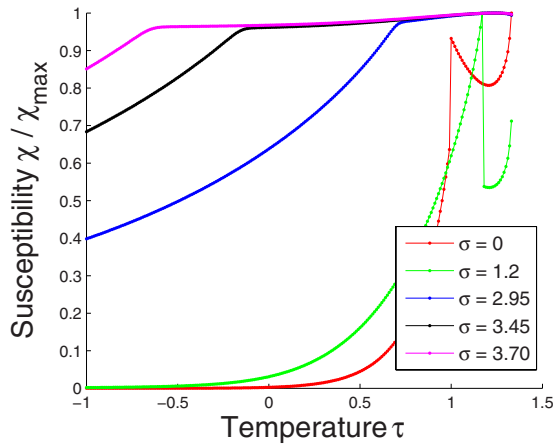

FIG. 2. (Color online) Normalized susceptibilities versus the temperature for different value of the disorder σ_J. Parameters (Refs. 6 and 21) appropriate for FePd are $\xi=0.5$, $E_0=3$, $T_0=1$, $T_c=0.9$, and $\sigma_\Delta=0$. Both the jump in the first-order phase transition and the second-order cusp are evident.
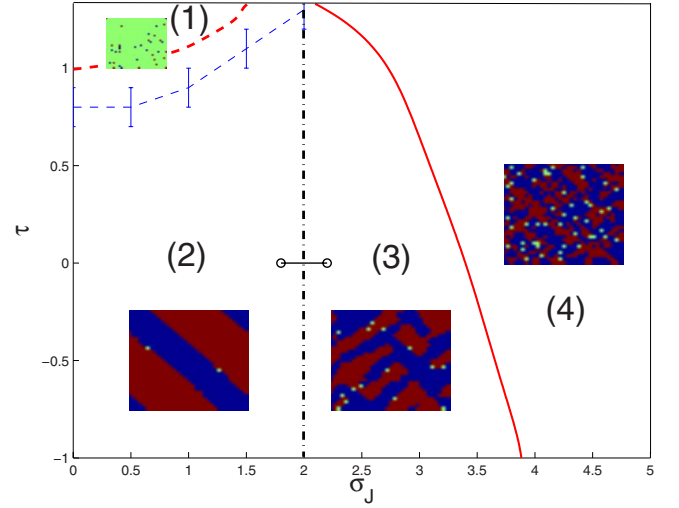

FIG. 3. (Color online) Phase diagram with results of Monte Carlo simulations with long-range interactions controlled by the stiffness, $A_1(\sigma_\Delta=0, A_1=4)$. The red curves are the mean-field transition lines for $A_1=0$. The dashed blue line with error bars is the first-order transition line, determined numerically, between (1) austenite and [(2) and (3)] martensite. The shape of this line does not quite have the experimentally observed dependence because we have added the disorder in the coefficient rather than in the temperature in the Hamiltonian (2). The martensite phase is separated by the vertical dash line into two metastable regions: (2) twins and (3) frustrated twins. The twins are stable for $\sigma_J < 2 \pm 0.2$. A glassy phase (4) still exists for nonzero, A_1, as confirmed by ZFC-FC experiments. The precise location of the glass transition between (3) and (4) requires detailed simulations.

function of the excess concentration of one of the constituents.

The Fig. 3 compares the phase diagram (and microstructure) obtained using Monte Carlo simulations for a nonzero value of the stiffness A_1, with the ratio $\frac{A_1}{A_3} = \frac{1}{2}$ for FePd, to the mean-field result. The simulations were carried out on a 32×32 lattice and the topology of the phase diagram is essentially the same as in Fig. 1 except that the martensite region is now split into two metastable phases consisting of twins and frustrated twins instead of a unique uniform phase given by mean-field theory. We also note that martensite transition temperature is lowered by long-range interactions, as seen in continuum simulations. However, we note that the mean-field predicts that disorder has the effect of increasing this transition temperature, rather than decreasing it, as has been noted experimentally.[1,4] This is a consequence of the way we have introduced disorder, in the coefficients rather than in the temperature. A direct Monte Carlo simulation of the model with disorder in the temperature, rather than in the coefficient, would be expected to correctly obtain this dependence, as is typically included in the harmonic strain term in the original continuum model.

Detailed studies are required to establish precisely where the transition to a glassy state occurs. Our Monte Carlo results are qualitative and the precise location of the transition lines requires further analysis. However, our results on larger lattices (64×64) show similar trends as do (Fig. 4) our more
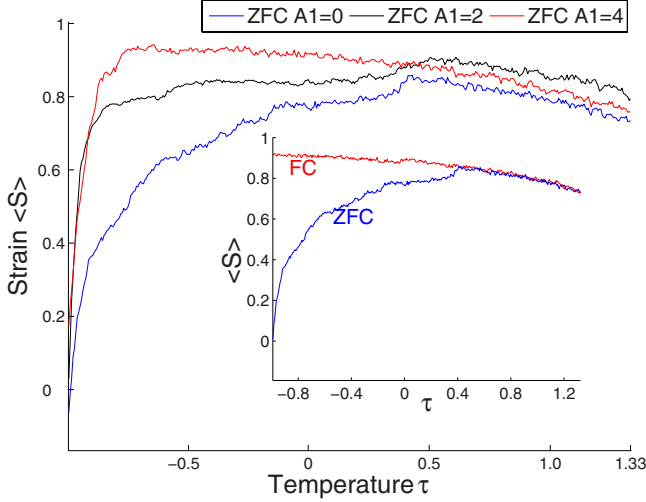
FIG. 4. (Color online) FC-ZFC results from Monte Carlo simulations for disorder $\sigma_J=4$, $\sigma_\Delta=0$, and for different strengths of the long-range interaction, A_1. The glassy behavior progressively disappears as we increase A_1, the repulsive compatibility potential favors long-range order that competes with the disorder. The inset shows ZFC-FC curves for $A_1=0$, σ_Δ, and $\sigma_J=4$, confirming the predictions of glassy behavior from the mean-field theory for these parameters.

quantitative FC-ZFC simulations[1,28] on the microstructure obtained in the glass phase. We have verified that for large-enough values of the disorder and no long-range interactions there is significant history dependence, confirming the mean-field result that long-range interactions are not necessary to obtain a strain glass phase. Moreover, the long-range interactions do not favor the glass phase and the glass transition is shifted to larger values of the disorder as we increase the elastic stiffness A_1. These curves are in good agreement with other numerical results based on Landau theory.[9]

We also studied the effects of an external field (stress), h, on the strain glass phase that was generated by adding disorder with $\sigma_J=3.5$. The external stress field is simply introduced by adding the term $-h\Sigma_i S_i$ to Hamiltonian (2), that leads to a term βh in γ in Eq. (6). Figure 5 shows that the external field favors the ordered martensite state. The trend is similar to that observed in $Ni_{48.5}Ti_{51.5}$ alloys where a thermodynamic phase boundary separates the martensite from the strain glass phase.[29] For comparison, we also show in the inset of Fig. 5 the behavior from the model of the effects of the field (stress) on a normal martensite transition temperature without any disorder. This shows that the critical field for stress-induced martensite decreases *linearly* as the temperature is lowered. This is consistent with the Clausius-Clapeyron equation, as also confirmed experimentally.[29]

IV. RANDOM-FIELD MODEL

We have also studied the effects of disorder through the addition of a random field, i.e., a random local field distributed according to a Gaussian distribution of zero mean-field value and of variance σ_h^2. We thus add a term $-\Sigma_i h_i S_i$ to Hamiltonian (2) with $\sigma_J=\sigma_\Delta=0$. The influence of a random
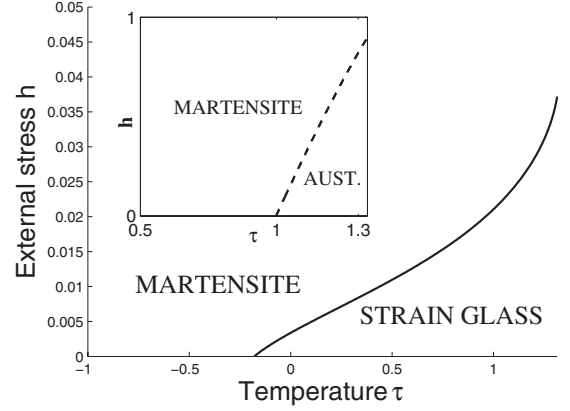

FIG. 5. Mean-field temperature-stress phase diagram with and without disorder. The inset is the phase diagram for a normal martensitic alloy without any disorder ($\sigma_J=0$). The first-order transition temperature increases linearly with the applied stress, as expected from the Clausius-Clapeyron equation. The phase diagram with disorder ($\sigma_J=3.5$) shows a strain glass phase in addition to the martensite, clearly indicating that the external field favors the latter. The two phase diagrams capture the salient behavior seen in experiments on $Ni_{48.5}Ti_{51.5}$ (Ref. 29).

field on a spin-1 model has already been studied for discrete distributions of the field[30,31] so that the self-consistency equation for m in this case is

$$m = \int \frac{dx}{\sqrt{2\pi}} e^{-x^2/2} \frac{2 \sinh(z\beta J_0 m + \beta\sigma_h x)}{e^{\beta\Delta_0} + 2 \cosh(z\beta J_0 m + \beta\sigma_h x)}, \quad (7)$$

and q can be independently calculated from the value of m. Figure 6 shows the phase diagram obtained for this model. We find an independent spin phase[30] characterized by the EA
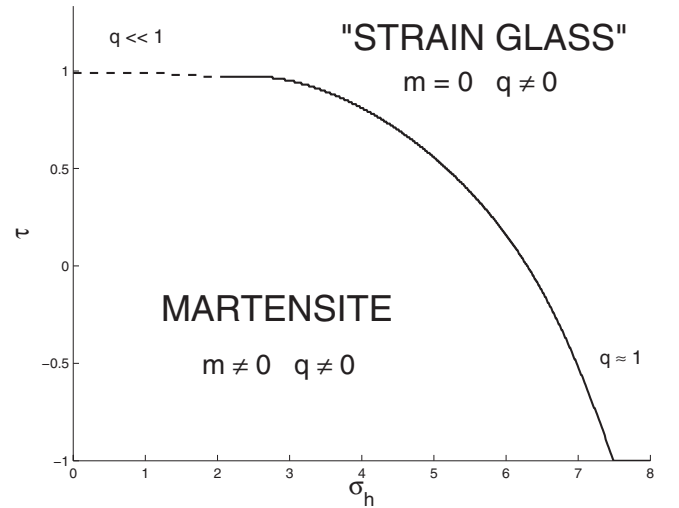

FIG. 6. Mean-field phase diagram for the random-field model containing the term $-\Sigma_i h_i S_i$. The austenite (paramagnetic) phase only exists for $\sigma_h=0$ and $\tau>1$. There are two other phases: martensite (ferromagnetic) and strain glass (independent spin). These two phases are separated by a first-order transformation (dashed line) and by a solid line of critical points that meet in a tricritical point.

order parameter. This phase is fundamentally different from the SK spin glass since the spins are not correlated,[30] but it has the features of glass, such as very slow dynamics.[32] Although there is no austenite phase for nonzero values of the disorder, the topology of the phase diagram is not so different from that obtained from the previous model. Hence, the method used to introduce randomness does not have a bearing on the essential features of the phase diagram.

V. CONCLUSION

In summary, we have demonstrated that a strain pseudospin model for the square to rectangle transformation predicts the existence of a strain glass phase in the presence of disorder. Our predicted phase diagram from mean-field theory and Monte Carlo simulations is consistent with the salient features of the experimental results obtained for many martensitic alloys. We have introduced disorder in several ways and our conclusions are quite robust. We find that the long-range elastic interaction is not necessary for the existence of the strain glass phase. It, however, competes with the disorder and moves the glass transition to higher temperatures. By examining the signature in the susceptibility, we predict a second-order phase transition from the martensitic ground state to the glass phase as a function of disorder, which can be experimentally confirmed by varying the alloy concentration. Our evaluated phase diagram tells us the properties the system would have if it relaxed toward equilibrium. Real systems would, of course, possess very slow dynamics such that it likely would not be able to reach equilibrium, but the phase transition may be described theoretically by equilibrium thermodynamics. The ZFC-FC curves and the phase diagrams in the temperature-stress plane are also consistent with measurements from experiments.

An improved model would consider disorder through the transition temperature T_0 that appears in τ rather than in the coefficients of the Hamiltonian. We expect the universal features of the glassy transition to remain true in this model. It would predict the correct decrease in the transition temperature as a function of the disorder, as constructed in the continuum theory. This model with Gaussian distribution of the disorder is probably too complex to be studied analytically. A simpler distribution,[33] such as $\mathcal{P}(T_0^i) = \frac{1}{2}\delta[T_0^i - (T_0+\sigma)] + \frac{1}{2}\delta[T_0^i - (T_0-\sigma)]$, with variance σ^2 could yield better agreement with experiments.

Our approach may be generalized to more complex transitions in 2D, such as the triangle-to-rectangle, or in 3D to the cubic-to-tetragonal transition. For these two cases, the glassy phase would correspond to a three-states clock glass, also known as Potts Glass.[34] It would also be interesting to investigate out-of-equilibrium properties of our model, both in the glassy phase[35] as well as near the first-order transition where one expects hysteresis[36] and history dependence.

Finally, our study provides the basis for investigating the rich and technologically relevant behavior that the strain glass phase shows, namely, the shape-memory effect in a new regime of the martensite phase diagram.[1]

APPENDIX: REPLICA STUDY OF THE RANDOM CRYSTAL FIELD–RANDOM INTERACTIONS MODEL

We consider the spin-1 Hamiltonian associated with the two-dimensional square-to-rectangle ferroelastic transformation in the limit $A_1=0$. It is given by the Eq. (2) where the J_{ij}'s and the Δ_i's are distributed according to Gaussian distributions as defined in the text. We wish to calculate the free energy averaged over the quenched disorder

$$-\beta F = \int \prod_i d\Delta_i \mathcal{P}(\Delta_i) \prod_{i,j} dJ_{ij} \mathcal{P}(J_{ij}) \ln Z[\{J_{ij}\}, \{\Delta_i\}]. \tag{A1}$$

To do so, we use the so-called replicas trick that relies on the identity $\overline{\ln Z} = \lim_{n\to 0} \frac{\overline{Z^n} - 1}{n}$, where the bar refers to an average over the disorder. For n integer, Z^n is the partition function of n identical systems, its average is

$$\overline{Z^n} = \int \prod_{i,j} dJ_{ij}\mathcal{P}(J_{ij}) \int \prod_i d\Delta_i \mathcal{P}(\Delta_i)$$
$$\times \mathrm{Tr}_n \exp\sum_\alpha \left(\beta\sum_{\langle i,j\rangle} J_{ij}S_i^\alpha S_j^\alpha - \beta\sum_i \Delta_i S_{i\alpha}^2\right), \tag{A2}$$

$$= \mathrm{Tr}_n \exp\left\{\beta J_0 \sum_\alpha \sum_{\langle i,j\rangle} S_i^\alpha S_j^\alpha - \beta\Delta_0 \sum_{i,\alpha} S_{i\alpha}^2 \right.$$
$$\left. + \frac{\beta^2}{2}\sum_{\alpha,\beta}\left(\sigma_J^2 \sum_{\langle i,j\rangle} S_i^\alpha S_i^\beta S_j^\alpha S_j^\beta + \sigma_\Delta^2 \sum_i S_{i\alpha}^2 S_{i\beta}^2\right)\right\}, \tag{A3}$$

where α and β label n dummy replicas and $\mathrm{Tr}_n\{\cdots\} = \Sigma_{\{S_i^1\}}\cdots\Sigma_{\{S_i^n\}}\{\cdots\}$ is the trace over all the spins. The last term represents effective interactions between the replicas. We can thus express the free energy as

$$\beta f = -\lim_{\substack{N\to\infty \\ n\to 0}} \frac{1}{Nn}\left\{\mathrm{Tr}_n \exp\left[\beta J_0 \sum_\alpha \sum_{\langle i,j\rangle} S_i^\alpha S_j^\alpha - \beta\Delta_0 \sum_{i,\alpha} S_{i\alpha}^2\right.\right.$$
$$\left.\left. + \frac{\beta^2}{2}\sum_{\alpha,\beta}\left(\sigma_J^2 \sum_{\langle i,j\rangle} S_i^\alpha S_i^\beta S_j^\alpha S_j^\beta + \sigma_\Delta^2 \sum_i S_{i\alpha}^2 S_{i\beta}^2\right)\right] - 1\right\}. \tag{A4}$$

Following the usual replica method, we treat the terms with $\alpha=\beta$ and the terms with $\alpha\neq\beta$ separately. That is, we write

$$\sum_{\langle i,j \rangle} \sum_{\alpha\beta} S_i^\alpha S_j^\alpha S_i^\beta S_j^\beta = \sum_{\langle i,j \rangle} \sum_\alpha S_{i\alpha}^2 S_{j\alpha}^2 + 2 \sum_{\langle i,j \rangle} \sum_{(\alpha\beta)} S_i^\alpha S_j^\alpha S_i^\beta S_j^\beta,$$

(A5)

where $(\alpha\beta)$ are different combinations of α and β. The replicated system trace in Eq. (A4) cannot be performed exactly, we thus introduce three mean-field parameters

$$m^\alpha = \langle S_i^\alpha \rangle_n, \quad p^\alpha = \langle S_{i\alpha}^2 \rangle_n, \quad q^{\alpha\beta} = \langle S_i^\alpha S_i^\beta \rangle_n (\alpha \neq \beta),$$

(A6)

where the brackets indicate statistical averages. We further make the usual replicas ansatz that all the m's, q's, and p's have the same value at the extremum of the free energy. Mean-field approximation consists in performing the replacements

$$\sum_\alpha \sum_{\langle i,j \rangle} S_i^\alpha S_j^\alpha \rightarrow z \sum_{i\alpha} \left(m S_i^\alpha - \frac{m^2}{2} \right),$$

(A7)

$$\sum_\alpha \sum_{\langle i,j \rangle} S_{i\alpha}^2 S_{j\alpha}^2 \rightarrow z \sum_{i\alpha} \left(p S_{i\alpha}^2 - \frac{p^2}{2} \right),$$

(A8)

$$\sum_{(\alpha\beta)} \sum_{\langle i,j \rangle} S_i^\alpha S_j^\alpha S_i^\beta S_j^\beta \rightarrow z \sum_i \sum_{(\alpha\beta)} \left(q S_i^\alpha S_i^\beta - \frac{q^2}{2} \right), \quad \text{(A9)}$$

where z is the number of nearest neighbors. Mean-field approximation yields the free energy

$$\beta f = -\lim_{n \to 0}^{N \to \infty} \frac{1}{Nn} \left(\text{Tr}_n \exp\left(\beta^2 \sigma_J^2 z \left[\sum_{i,(\alpha\beta)} q S_i^\alpha S_i^\beta \right. \right. \right.$$
$$\left. - \frac{Nn(n-1)}{4} q^2 + 2 \sum_{i\alpha} p S_{i\alpha}^2 - \frac{nN}{2} p^2 \right]$$
$$+ \beta J_0 z m \left(\sum_{i\alpha} S_i^\alpha - \frac{nN}{2} m^2 \right) - \Delta_0 \sum_{i\alpha} S_{i\alpha}^2$$
$$\left. \left. + \frac{\beta \sigma_\Delta}{2} \sum_i \left(\sum_\alpha S_i^\alpha \right)^2 \right) - 1 \right).$$

(A10)

Writing $\sum_{(\alpha\beta)} q S_i^\alpha S_i^\beta = q/2[(\sum_\alpha S_i^\alpha)^2 - \sum_\alpha S_{i\alpha}^2]$ and using the Hubbard Stratonovich identity Gaussian identity $\exp(\frac{a^2}{2}) = \int_{-\infty}^{+\infty} \frac{dx}{\sqrt{2\pi}} \exp(-\frac{x^2}{2} + ax)$ for the quadratic terms, one obtains the mean-field free energy Eq. (5). Minimizing the free energy yields the self-consistency equations (see text). It is also straightforward to show that in the original system $m = \overline{\langle S \rangle}$, $q = \overline{\langle S \rangle^2}$, and $p = \overline{\langle S^2 \rangle}$.

---

[1] S. Sarkar, X. Ren, and K. Otsuka, Phys. Rev. Lett. **95**, 205702 (2005); Y. Wang, X. Ren, and K. Otsuka, *ibid.* **97**, 225703 (2006); Mater. Sci. Forum **583**, 67 (2008).

[2] J. A. Mydosh, *Spin Glasses* (Taylor & Francis, London, 1993).

[3] D. Viehland and Y.-H. Chen, J. Appl. Phys. **88**, 6696 (2000); D. Viehland, J. F. Li, S. J. Jang, L. E. Cross, and M. Wuttig, Phys. Rev. B **46**, 8013 (1992).

[4] X. Ren *et al.*, Philos. Mag. **90**, 141 (2010).

[5] S. Kartha, T. Castán, J. A. Krumhansl, and J. P. Sethna, Phys. Rev. Lett. **67**, 3630 (1991).

[6] S. Kartha, J. A. Krumhansl, J. P. Sethna, and L. K. Wickham, Phys. Rev. B **52**, 803 (1995).

[7] J. P. Sethna, S. Kartha, T. Castán, and J. A. Krumhansl, Phys. Scr. **T42**, 214 (1992).

[8] D. Sherrington, J. Phys.: Condens. Matter **20**, 304213 (2008).

[9] P. Lloveras, T. Castán, M. Porta, A. Planes, and A. Saxena, Phys. Rev. Lett. **100**, 165707 (2008); Phys. Rev. B **80**, 054107 (2009).

[10] S. R. Shenoy and T. Lookman, Phys. Rev. B **78**, 144103 (2008).

[11] R. Vasseur, T. Lookman, and S. R. Shenoy (unpublished); S. R. Shenoy *et al.* (unpublished); N. Shankaraiah *et al.* (unpublished).

[12] S. F. Edwards and P. W. Anderson, J. Phys. F: Met. Phys. **5**, 965 (1975).

[13] D. Sherrington and S. Kirkpatrick, Phys. Rev. Lett. **35**, 1792 (1975).

[14] S. K. Ghatak and D. Sherrington, J. Phys. C **10**, 3149 (1977).

[15] A. Crisanti and L. Leuzzi, Phys. Rev. B **70**, 014409 (2004).

[16] M. Blume, Phys. Rev. **141**, 517 (1966); H. W. Capel, Physica (Amsterdam) **32**, 966 (1966); M. Blume, V. J. Emery, and R. B.

Griffiths, Phys. Rev. A **4**, 1071 (1971).

[17] S. Muto, R. Oshima, and F. E. Fujita, Acta Metall. Mater. **38**, 685 (1990).

[18] A. Saxena and G. R. Barsch, Physica D **66**, 195 (1993).

[19] G. R. Barsch, Mater. Sci. Forum **327**, 367 (2000).

[20] K. Otsuka and X. Ren, Prog. Mater. Sci. **50**, 511 (2005).

[21] T. Lookman, S. R. Shenoy, K. Ø. Rasmussen, A. Saxena, and A. R. Bishop, Phys. Rev. B **67**, 024114 (2003).

[22] G. A. Saunders, Phys. Scr. **T1**, 49 (1982).

[23] M. Baus and R. Lovett, Phys. Rev. Lett. **65**, 1781 (1990); Phys. Rev. A **44**, 1211 (1991).

[24] X. Campi and H. Krivine, Europhys. Lett. **66**, 527 (2004).

[25] G. Parisi, J. Phys. A **13**, 1101 (1980).

[26] G. Parisi, Phys. Rev. Lett. **43**, 1754 (1979).

[27] M. Mezard, G. Parisi, and M. A. Virasoro, *Spin Glass Theory and Beyond* (World Scientific, Singapore, 1987).

[28] Y. Wang, X. Ren, K. Otsuka, and A. Saxena, Phys. Rev. B **76**, 132201 (2007).

[29] Y. Wang, X. Ren, K. Otsuka, and A. Saxena, Acta Mater. **56**, 2885 (2008).

[30] T. Schneider and E. Pytte, Phys. Rev. B **15**, 1519 (1977).

[31] M. Kaufman and M. Kanner, Phys. Rev. B **42**, 2378 (1990).

[32] P. Young, *Spin Glasses and Random Fields* (World Scientific, Singapore, 1998).

[33] A. Benyoussef, T. Biaz, M. Saber, and M. Touzani, J. Phys. C **20**, 5349 (1987).

[34] D. J. Gross, I. Kanter, and H. Sompolinsky, Phys. Rev. Lett. **55**, 304 (1985).

[35] L. F. Cugliandolo and J. Kurchan, J. Phys. A **27**, 5749 (1994).

[36] B. Cerruti and E. Vives, Phys. Rev. B **77**, 064114 (2008).